Supporting Information

Homo- and Heterobimetallic Ruthenium(II) and Osmium(II) Complexes Based on a Pyrene-Biimidazolate Spacer as Efficient DNA-Binding Probes in the Near-Infrared Domain

Sourav Mardanya, Srikanta Karmakar, Debiprasad Mondal, and Sujoy Baitalik*

Department of Chemistry, Inorganic Chemistry Section, Jadavpur University, Kolkata – 700032, India

Physical Measurements. Elemental analyses of the compounds were performed with a Vario-Micro V2.0.11 elemental (CHNSO) analyzer. NMR spectra were collected on either a Bruker 300 or Bruker 500 spectrometer in DMSO-d_6, and high resolution mass spectroscopy was performed on a Waters Xevo G2 QTOf mass spectrometer. The UV/vis absorption spectra were recorded with a Shimadzu UV 1800 spectrometer. A matched pair of quartz cuvettes (path length 1 cm) was employed. Steady state luminescence spectra were obtained either by a Perkin–Elmer LS55 or Spex fluorolog-2 spectrofluorometer equipped with DM3000F software. Luminescence quantum yields were determined by using literature method taking $[Ru(bpy)_3]^{2+}$ as the standard. Luminescence lifetime measurements were carried out by using time–correlated single photon counting set up from Horiba Jobin-Yvon. The luminescence decay data were collected on a Hamamatsu MCP photomultiplier (R3809) and were analyzed by using IBH DAS6 software. Cyclic and square-wave voltammetric experiments were performed in deaerated acetonitrile with a BAS epsilon electrochemistry system and a three-electrode set up consisting of a platinum or glassy carbon working electrode, a platinum counter electrode, and Ag/AgCl reference electrode. Tetraethylammonium perchlorate (TEAP) was used as background electrolyte. The potentials reported in this study were referenced against the Ag/AgCl electrode, which under the given experimental conditions gave a value of 0.36 V for the Fc/Fc^+ couple.

DNA Binding Experiments

Absorption and Emission Spectral Experiments. UV-vis absorption and emission titrations were carried out by maintaining a constant metal complex concentration (20 μM) and adding incrementally the CT-DNA solution of appropriate concentration in 5 mM Tris-HCl/ NaCl buffer with the ionic strength of 50 .0 × 10^{-3} m (pH 7.30) at room temperature. After each addition of DNA to the solution of the metal complexes, the resulting solution was allowed to equilibrate at 25 °C for 5 min, after which the absorption and emission readings were noted. Proper corrections were made to the absorbance of CT-DNA. The equilibrium binding constant (K_b) and the binding site size (s, per base pair) of the complexes to CT-DNA were calculated by non-linear least square analysis of the isotherm using the expression of Bard and co-workers based on the McGhee-von Hippel (MvH) model.[S1-S2]

$$(\varepsilon_a - \varepsilon_f)/(\varepsilon_b - \varepsilon_f) = (b - (b^2 - 2K_b{}^2C_t[DNA]/s)^{1/2})/2K_bC_t \quad \text{(S1)}$$

$$(I_a - I_f)/(I_b - I_f) = (b - (b^2 - 2K_b{}^2C_t[DNA]/s)^{1/2})/2K_bC_t \quad \text{(S2)}$$

where b = 1 + K_bC_t + K_b[DNA]/2s, ε_a is the extinction coefficient observed for the spectral band at a given DNA concentration, ε_f is the extinction coefficient of the free complex in solution, ε_b is the extinction coefficient of the complex when fully bound to DNA. Similarly I_a, I_f and I_b are the luminescence intensities of the complex at a given DNA concentration, free complex and fully bound to DNA respectively. K_b is the equilibrium binding constant, C_t is the total complex concentration, [DNA] is the DNA concentration in nucleotides and s is the binding site size of the complexes in base pairs. The non-linear least-square fit analysis was done using Origin Lab software. The lifetimes of the complexes were also recorded as a function of CT-DNA in 5 mM Tris-HCl/ NaCl buffer with the ionic strength of 50 .0 × 10^{-3} m (pH 7.30) at room temperature.

Competitive Binding Fluorescence Experiments. The apparent binding constants (K_{app}) of the complexes have been evaluated by using ethidium bromide (EB)-bound CT-DNA solution in 5 mM Tris-HCl/ NaCl buffer with the ionic strength of 50 .0 × 10^{-3} m (pH 7.30) at room temperature. The luminescence intensities at 602 nm (546 nm excitation) of EB-DNA conjugate with increasing concentration of **1, 2** and **3** were recorded. The K_{app} values were calculated by using the equation K_{EB} × [EB] = K_{app} × [complex], where K_{EB} is the binding constant of EB (K_{EB} = 1.25 × 10^6 M^{-1}), [EB] is the concentration of EB (13 μM) and [complex] is the concentration of the complex at 50% reduction of the initial fluorescence emission intensity.[S3]

Circular Dichroism Experiments. The Circular dichroism (CD) spectroscopy was studied on a JASCO J-815 CD spectropolarimeter between 400 and 200 nm in continuous scanning mode at 25°C. Experiments were performed by adding progressively increasing amounts of complexes (**1**, **2** and **3**) to the solutions of CT-DNA [40μM] in 5 mM Tris-HCl/ NaCl buffer with the ionic strength of 50 .0 × 10^{-3} m (pH 7.30).

X-ray Crystallographic Analyses. The crystallographic data, details of data collection, and refinement parameter for the complexes **1** and **2** were summarized in Table S1. In each case, single crystals of suitable size were obtained by diffusing toluene to 1:1 acetonitrile-dichlorometane solution of the complexes. The crystals were immersed in paratone oil and then mounted on the tip of a glass fiber and cemented using epoxy resin. Intensity data for these crystals were collected using MoKα (λ = 0.7107 Å) radiation on a Bruker SMART APEX II diffractometer equipped with CCD area detector at room temperature. The data integration and reduction were processed with SAINT[S4] software provided with the software package of SMART APEX II. An empirical absorption correction was applied to the collected reflections with SADABS.[S4] The structures were solved by direct

methods using SHELXTL [S5] and were refined on F^2 by the full-matrix least-squares technique using the SHELXL-97 [S6] program package. Graphics were generated using PLATON. [S7] In both cases, the non-hydrogen atoms were refined anisotropically until the convergence. All the hydrogen atoms were geometrically positioned and treated as riding atoms. In both complexes **1** and **2**, the hydrogen atoms of the lattice water molecules could not be located from the difference Fourier map.

CCDC reference numbers are 1439503 for **1** and 1439504 for **2.**

Theoretical Computational Methods. Quantum chemical calculations were performed with the Gaussian 09 program [S8] employing the DFT method with Becke's three-parameter hybrid functional and Lee-Yang-Parr's gradient corrected correlation functional B3LYP level of theory.[S9-S10] The 6-31G(d) basis set was employed for the C, H and N while SDD basis set was used for Ru and Os atoms. [S11] Geometries were fully optimized using the criteria of the respective programs. To compute the UV-vis transition of the compounds, the singlet excited state geometries corresponding to the vertical excitations were optimized using the time-dependent DFT (TDDFT) scheme starting with the ground state geometries optimized in solution phase.[S12-S15] The excitation energies, computed within the acetonitrile solvent simulated by the CPCM model,[S16] has been determined by using the so-called nonequilibrium approach, which has been designed for the study of the absorption process.[S17-S18] Only singlet-singlet transitions, that is, the spin-allowed transitions, have been taken into account. UKS calculations were also performed directly on triplet state of the complexes to calculate singlet-triplet energy gap in CH_3CN using the CPCM model. Orbital analysis was completed with Gauss View[S19] and Gauss sum 2.2.[S20]

Table S1. Crystallographic Data for Complex **1** and **2**

Crystallographic table		
	1	**2**
formula	C_{60} H_{42} N_{12} Ru_2Cl_2 O_8	C_{67} H_{50} Cl_2 N_{12} O_8 Os_2
fw	1332.10	1602.55
T (K)	273(2)	273(2)
Cryst syst	Monoclinic	Monoclinic
Space group	P2(1)/n	P2(1)/n
a (Å)	11.7951(6)	11.8080(4)
b (Å)	27.9283(13)	27.8673(9)
c (Å)	23.3331(12)	23.4456(8)
α (deg)	90	90
β (deg)	100.952(3)	101.537(2)
γ (deg)	90	90
V (Å^3)	7546.3(6)	7559.1(4)
Dc(g cm^{-3})	1.172	1.367
Z	4	4
μ (mm^{-1})	0.522	3.483
F(000)	2688.0	3068.0
θ range (deg)	2.24-25.00	2.25-27.00
data/restraints/params	13287/0/757	16473/0/809
GOF on F^2	1.029	0.941
R1[a] [$I > 2\sigma(I)$], wR2 [b](all data)	0.0831 0.2363	0.0616 0.1438
$\Delta\rho_{max}/\Delta\rho_{min}$ (e Å)	2.362/-0.394	1.004/-1.061

[a]$R1(F) = [\sum || F_0 | - |F_C || / \sum | F_0]$, [b]$wR2\ (F^2) = [\sum w(F_0^2 - F_C^2)^2 / \sum w(F_0^2)^2]^{1/2}$

Table S2. Selected Calculated Bond Distances (Å) for **1**, **2** and **3** in Ground State and UKS State Along with Available X-ray Crystal Data

	1				**2**				**3**	
	Expt	Soln.(1)	uks.(1)		Expt	Soln.(2)	uks.(2)		Soln.(3)	uks(3)
Ru1-N7	2.022(7)	2.072	2.104	Os1-N7	2.033(7)	2.084	2.071	Ru1-N7	2.080	2.082
Ru1-N8	2.032(6)	2.054	2.070	Os1-N8	2.014(6)	2.063	2.068	Ru1-N8	2.060	2.058
Ru1-N5	2.043(6)	2.081	2.081	Os1-N5	2.033(7)	2.087	2.109	Ru1-N5	2.088	2.084
Ru1-N6	2.046(6)	2.087	2.084	Os1-N6	2.039(7)	2.097	2.128	Ru1-N6	2.093	2.096
Ru1-N1	2.118(6)	2.137	2.108	Os1-N1	2.11196)	2.153	2.092	Ru1-N1	2.145	2.155
Ru1-N3	2.198(6)	2.298	2.242	Os1-N3	2.191(6)	2.293	2.284	Ru1-N3	2.306	2.317
Ru2-N12	2.013(6)	2.054	2.059	Os2-N12	2.010(6)	2.063	2.062	Os1-N12	2.065	2.070
Ru2-N10	2.030(6)	2.087	2.097	Os2-N10	2.050(7)	2.097	2.099	Os1-N10	2.097	2.127
Ru2-N11	2.042(6)	2.072	2.082	Os2-N11	2.046(7)	2.084	2.087	Os1-N11	2.084	2.072
Ru2-N9	2.045(6)	2.081	2.087	Os2-N9	2.037(7)	2.087	2.084	Os1-N9	2.089	2.111
Ru2-N2	2.110(6)	2.137	2.147	Os2-N2	2.093(7)	2.153	2.161	Os1-N2	2.146	2.086
Ru2-N4	2.205(6)	2.298	2.310	Os2-N4	2.223(7)	2.293	2.302	Os1-N4	2.284	2.273

Table S3. Selected Calculated Bond Angles (Å) for **1**, **2** and **3** in Ground State and UKS State Along with Available X-ray Crystal Data

	1				**2**				**3**	
	Expt	Soln.(1)	uks(1)		Expt	Soln.(2)	uks(2)		Soln.(3)	uks.(3)
N7-Ru1-N8	79.1(3)	78.8	78.2	N7-Os1-N8	79.3(3)	78.0	79.1	N7-Ru1-N8	78.6	78.7
N7-Ru1-N5	98.1(3)	97.7	98.5	N7-Os1-N5	98.4(3)	98.6	97.0	N7-Ru1-N5	97.9	97.8
N8-Ru1-N5	92.5(2)	88.9	85.9	N8-Os1-N5	89.0(3)	88.8	85.7	N8-Ru1-N5	89.0	89.3
N7-Ru1-N6	176.8(3)	175.4	175.8	N7-Os1-N6	177.1(3)	175.6	173.7	N7-Ru1-N6	175.4	175.4
N8-Ru1-N6	99.1(3)	98.7	98.2	N8-Os1-N6	100.5(3)	99.6	99.9	N8-Ru1-N6	98.8	98.8
N5-Ru1-N6	79.2(3)	78.2	78.8	N5-Os1-N6	78.7(3)	77.5	76.6	N5-Ru1-N6	78.0	78.1
N7-Ru1-N1	88.2(2)	88.9	87.3	N7-Os1-N1	87.5(3)	88.4	89.5	N7-Ru1-N1	88.8	88.6
N8-Ru1-N1	87.5(2)	90.7	92.4	N8-Os1-N1	89.2(3)	91.4	91.4	N8-Ru1-N1	90.9	91.1
N5-Ru1-N1	173.6(3)	173.0	173.4	N5-Os1-N1	173.4(3)	172.7	172.1	N5-Ru1-N1	173.0	173.4
N6-Ru1-N1	94.4(3)	94.8	95.1	N6-Os1-N1	95.4(3)	95.3	96.6	N6-Ru1-N1	95.0	95.3
N7-Ru1-N3	95.7(3)	94.7	96.9	N7-Os1-N3	95.1(3)	95.4	96.8	N7-Ru1-N3	95.1	95.5
N8-Ru1-N3	167.4(2)	168.5	171.8	N8-Os1-N3	168.2(2)	168.3	170.2	N8-Ru1-N3	168.8	169.3
N5-Ru1-N3	99.7(2)	101.4	101.3	N5-Os1-N3	102.2(2)	101.7	103.6	N5-Ru1-N3	101.0	100.4
N6-Ru1-N3	86.7(2)	88.2	86.8	N6-Os1-N3	85.6(2)	87.4	85.0	N6-Ru1-N3	87.8	87.4
N1-Ru1-N3	80.8(2)	79.5	80.7	N1-Os1-N3	80.1(2)	78.6	79.6	N1-Ru1-N3	79.5	79.5
N12-Ru2-N10	99.0(2)	101.6	98.7	N12-Os2-N10	100.8(3)	99.6	99.5	N12-Os1-N10	99.6	99.9
N12-Ru2-N11	80.2(3)	78.8	78.7	N12-Os2-N11	78.5(3)	78.0	78.0	N12-Os1-N11	78.0	79.0
N10-Ru2-N11	177.3(3)	175.4	175.3	N10-Os2-N11	177.3(3)	175.6	175.5	N10-Os1-N11	175.5	173.8
N12-Ru2-N9	88.5(2)	88.9	88.9	N12-Os2-N9	93.6(2)	88.8	89.0	N12-Os1-N9	88.6	85.5
N10-Ru2-N9	79.4(3)	78.2	78.1	N10-Os2-N9	78.4(3)	77.5	77.5	N10-Os1-N9	77.4	76.6
N11-Ru2-N9	98.0(3)	97.7	97.8	N11-Os2-N9	99.1(3)	98.6	98.5	N11-Os1-N9	98.6	97.2
N12-Ru2-N2	89.5(2)	90.7	91.1	N12-Os2-N2	87.1(2)	91.4	91.6	N12-Os1-N2	91.4	91.5
N10-Ru2-N2	94.6(2)	94.8	95.4	N10-Os2-N2	95.3(3)	95.3	95.6	N10-Os1-N2	95.3	96.6
N11-Ru2-N2	88.0(2)	88.9	88.5	N11-Os2-N2	87.2(2)	88.4	88.2	N11-Os1-N2	88.5	89.4
N9-Ru2-N2	173.3(2)	173.0	173.5	N9-Os2-N2	173.7(3)	172.7	173.1	N9-Os1-N2	172.6	172.0
N12-Ru2-N4	168.4(2)	168.5	168.9	N12-Os2-N4	167.3(2)	168.3	168.8	N12-Os1-N4	168.1	170.1
N10-Ru2-N4	86.7(2)	88.2	87.7	N10-Os2-N4	85.8(3)	87.4	87.1	N10-Os1-N4	87.4	85.1
N11-Ru2-N4	94.6(3)	94.7	95.4	N11-Os2-N4	95.4(3)	95.4	95.8	N11-Os1-N4	95.4	96.8
N9-Ru2-N4	102.5(2)	101.4	101.2	N9-Os2-N4	98.4(2)	101.7	101.2	N9-Os1-N4	102.2	103.9
N2-Ru2-N4	79.9(2)	79.5	79.2	N2-Os2-N4	81.5(2)	78.6	78.6	N2-Os1-N4	78.4	79.4

Table S4. Fractional Intensities of Short and Long Components of **1** and **3**

		Fractional Intensities(α)	
Compound		α_1	α_2
Ru-Ru(1)		0.71	0.28
Ru-Os(3)	Ru-center	0.78	0.21
	Os-center	0.79	0.20

Table S5. Selected Molecular Orbital Along with their Energies and Compositions for **1- 3** in Solution Phase

	Energy/ eV		(%) Composition			
			1(%) Composition			
MO	**1**		Ru^{II}	pyrene imida	imida	bpy
LUMO+3	-2.35		7.65	0.31	0.05	91.96
LUMO+2	-2.38		7.65	0.37	0.09	91.87
LUMO+1	-2.42		4.23	0.21	0.26	95.29
LUMO	-2.44		3.70	0.28	0.35	95.64
HOMO	-4.97		8.93	69.18	20.80	1.07
HOMO-1	-5.48		74.35	0.69	13.24	11.70
HOMO-2	-5.58		65.64	24.81	0.06	9.46
HOMO-3	-5.63		72.89	10.97	2.25	13.87
			2(%) Composition			
MO	**2**		Os^{II}	pyrene imida	imida	bpy
LUMO+3	-2.28		9.78	0.33	0.09	89.77
LUMO+2	-2.31		9.68	0.43	0.17	89.70
LUMO+1	-2.39		5.67	0.39	0.32	93.60
LUMO	-2.42		4.81	0.47	0.52	94.17
HOMO	-4.97		19.51	58.89	18.57	3.01
HOMO-1	-5.24		74.51	0.24	11.18	14.05
HOMO-2	-5.37		69.19	17.56	0.27	12.96
HOMO-3	-5.43		67.21	13.51	2.41	16.85
			3(%) Composition				
MO	**3**		Ru^{II}	Os^{II}	pyrene imida	imida	bpy
LUMO+3	-2.28		0.56	9.03	0.38	0.11	89.90
LUMO+2	-2.34		6.45	0.74	0.32	0.08	92.38
LUMO+1	-2.38		1.94	2.80	0.29	0.29	94.65
LUMO	-2.41		1.64	2.48	0.36	0.41	95.08
HOMO	-4.95		2.80	13.33	61.88	19.56	2.40
HOMO-1	-5.31		11.13	58.13	7.73	9.99	13.00
HOMO-2	-5.43		9.11	58.75	18.27	1.25	12.60
HOMO-3	-5.55		27.67	44.97	3.50	3.32	20.51

Table S6. Phosphorescence Emission of the Complexes **1-3** in Acetonitrile According to UKS-Calculations and Associated Experimental Values

	Energy for singlet state (*E*1/Hartree)	Energy for triplet state (*E*2/Hartree)	Emission energy ΔE=(*E*2- *E*1)/ (eV)	λemission (theo)/nm	λemission (expt)/nm
1	-3158.6240	-3158.5586	1.77	696	719
2	-3150.2064	-3150.1487	1.57	790	827
3	-3154.4161	-3154.3591	1.55	799	820

Table S7. Selected Molecular Orbital Along with their Energies and Compositions for **1- 3** in UKS Optimised State

	Energy/ eV		(%) Composition			
			1(%) Composition			
MO	**1**		Ru^{II}	pyrene imida	imida	bpy
LUMO+3	-2.33		6.69	0.26	0.06	92.97
LUMO+2	-2.36		5.51	0.05	0.19	94.23
LUMO+1	-2.39		3.54	0.23	0.26	95.95
LUMO	-2.66		6.31	0.52	0.11	93.03
HOMO	-4.91		9.72	67.36	21.79	1.11
HOMO-1	-5.47		75.54	2.12	11.98	10.34
HOMO-2	-5.56		65.43	23.44	1.19	9.91
HOMO-3	-5.63		72.12	13.08	2.24	12.54
			2(%) Composition			
MO	**2**		Os^{II}	pyrene imida	imida	bpy
LUMO+3	-2.29		9.53	0.34	0.12	89.99
LUMO+2	-2.32		8.30	0.57	0.14	90.97
LUMO+1	-2.41		5.19	0.40	0.39	93.99
LUMO	-2.67		7.76	0.17	0.52	91.53
HOMO	-4.94		25.17	52.46	17.90	4.44
HOMO-1	-5.18		67.94	6.49	12.04	13.52
HOMO-2	-5.38		69.77	17.14	0.52	12.55
HOMO-3	-5.42		65.53	16.00	2.70	15.76
			3(%) Composition				
MO	**3**		Ru^{II}	Os^{II}	pyrene imida	imida	bpy
LUMO+3	-2.30		0.60	7.56	0.53	0.10	91.20
LUMO+2	-2.34		6.37	0.61	0.31	0.08	92.61
LUMO+1	-2.40		3.46	0.09	0.22	0.26	95.93
LUMO	-2.66		0.06	7.78	0.17	0.52	91.45
HOMO	-4.92		1.59	23.10	52.11	18.73	4.45
HOMO-1	-5.23		9.58	47.82	19.60	11.33	11.64
HOMO-2	-5.45		9.50	58.84	20.00	1.03	10.60
HOMO-3	-5.55		28.42	44.18	2.52	3.91	20.94

Table S8. Changes in Lifetime Values of **1-3** in presence of Increasing DNA Concentration

Compound	Lifetime Changes in Presence of DNA
1	τ_1 = 5.6→5.5 τ_2 = 13.6→26.5
2	τ_1 = 0.1→0.4 τ_2 = 1.1→3.6
3	τ_1 = 0.4→1.1 τ_2 = 2.8→5.1

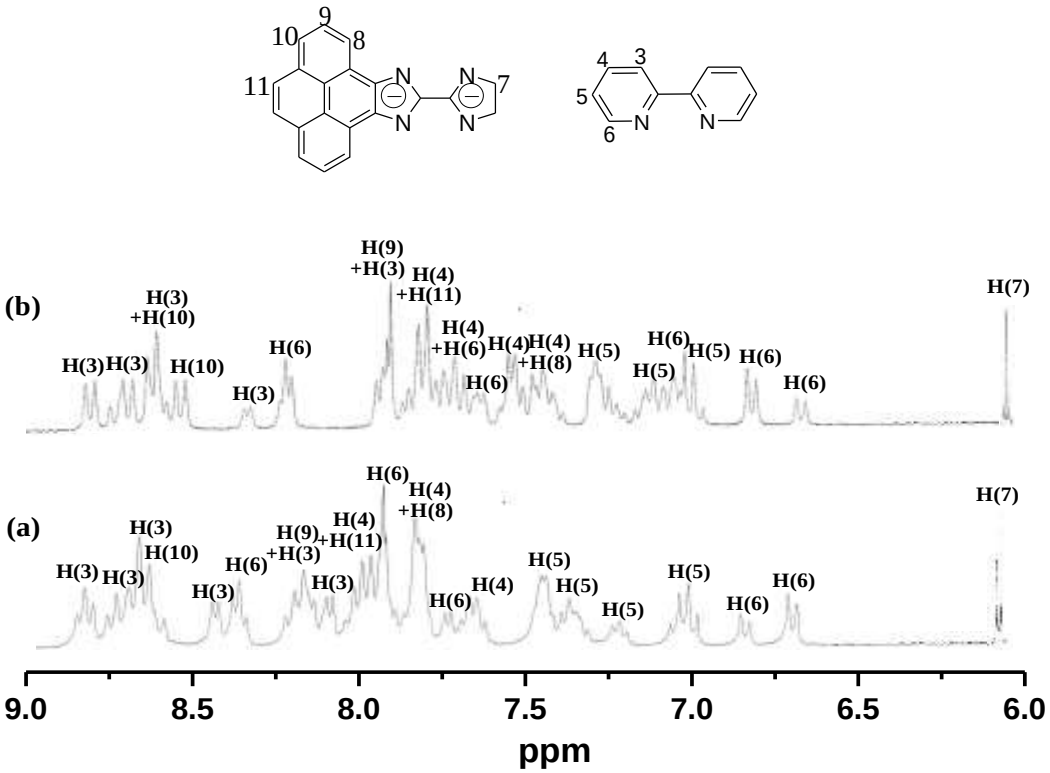

Figure S1. ^{1}H NMR spectra of complex **1** (a) and **2** (b) (300 MHz) in DMSO-d_6.

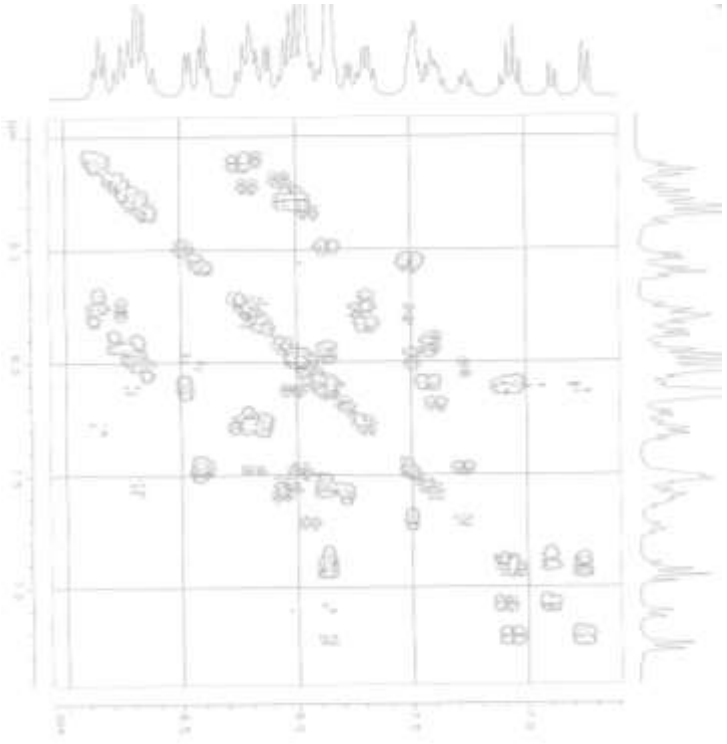

Figure S2. ^{1}H-^{1}H COSY NMR spectrum of **1** in DMSO-d_6.

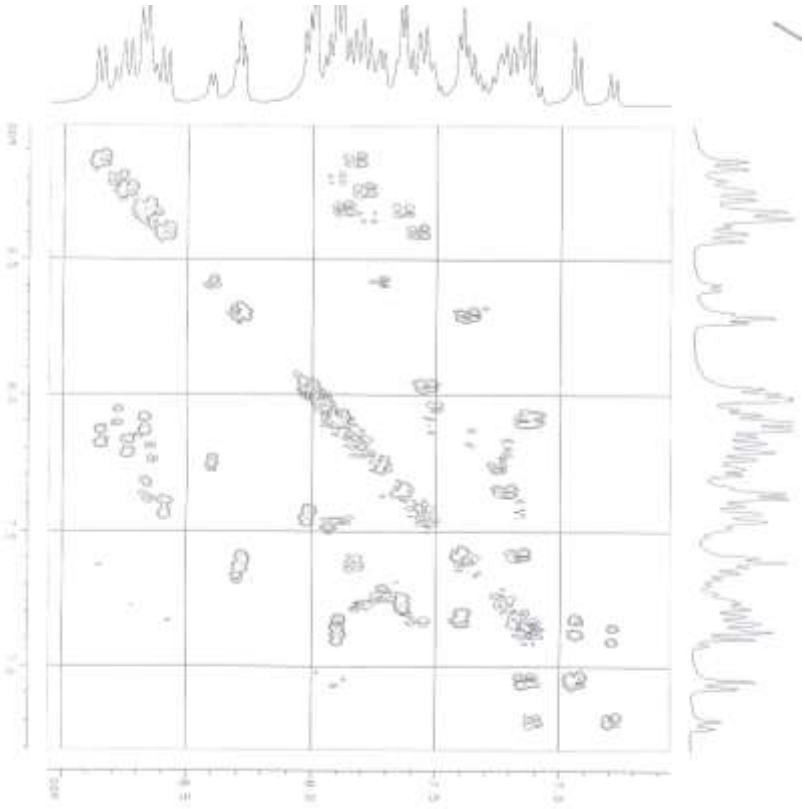

Figure S3. ^{1}H-^{1}H COSY NMR spectrum of **2** in DMSO-d_6.

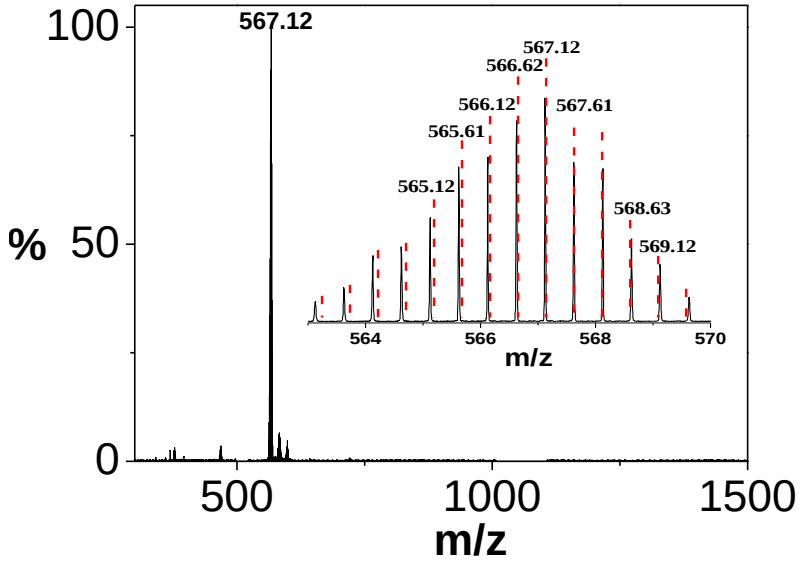

Figure S4. ESI-MS (positive) for the complex cations $[(bpy)_2Ru(Py\text{-}biimz)Ru(bpy)_2]^{2+}$ (*m/z* = 567.12) in acetonitrile showing the observed and isotopic distribution patterns.

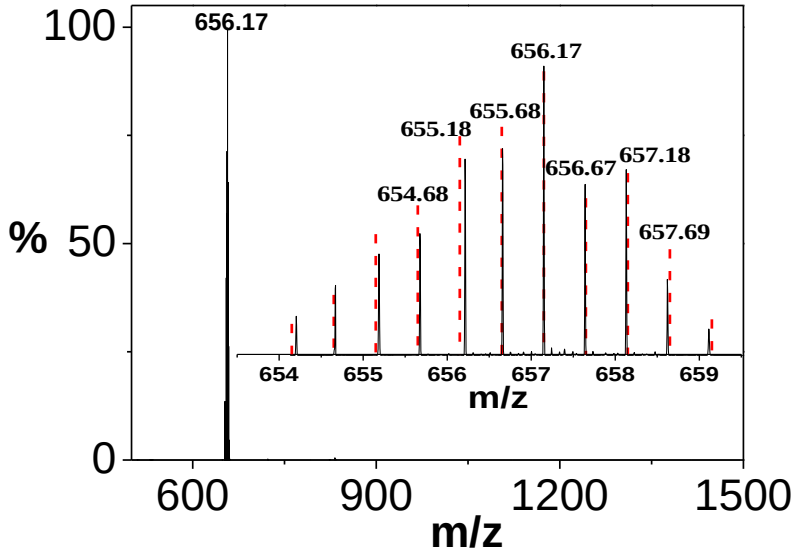

Figure S5. ESI-MS (positive) for the complex cations $[(bpy)_2Os(Py\text{-}biimz)Os(bpy)_2]^{2+}$ (*m/z* = 656.17) in acetonitrile showing the observed and isotopic distribution patterns.

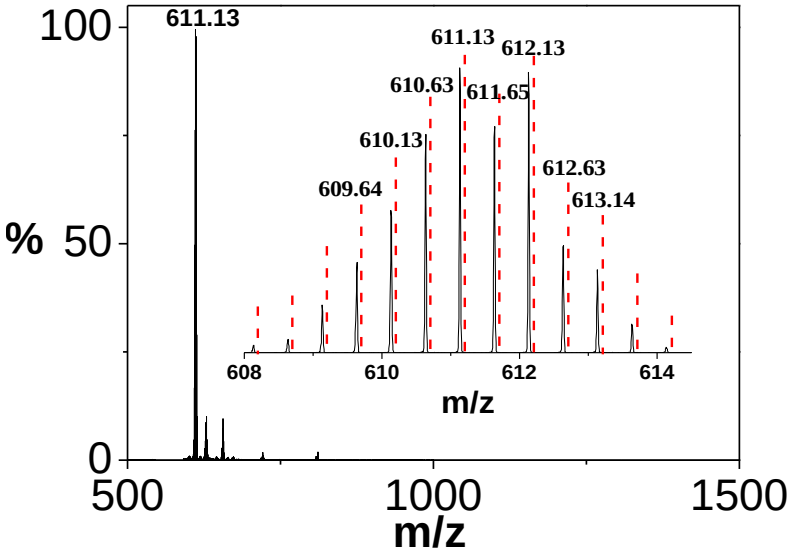

Figure S6. ESI-MS (positive) for the complex cations $[(bpy)_2Ru(Py\text{-}biimz)Os(bpy)_2]^{2+}$ (*m/z* = 611.13) in acetonitrile showing the observed and isotopic distribution patterns.

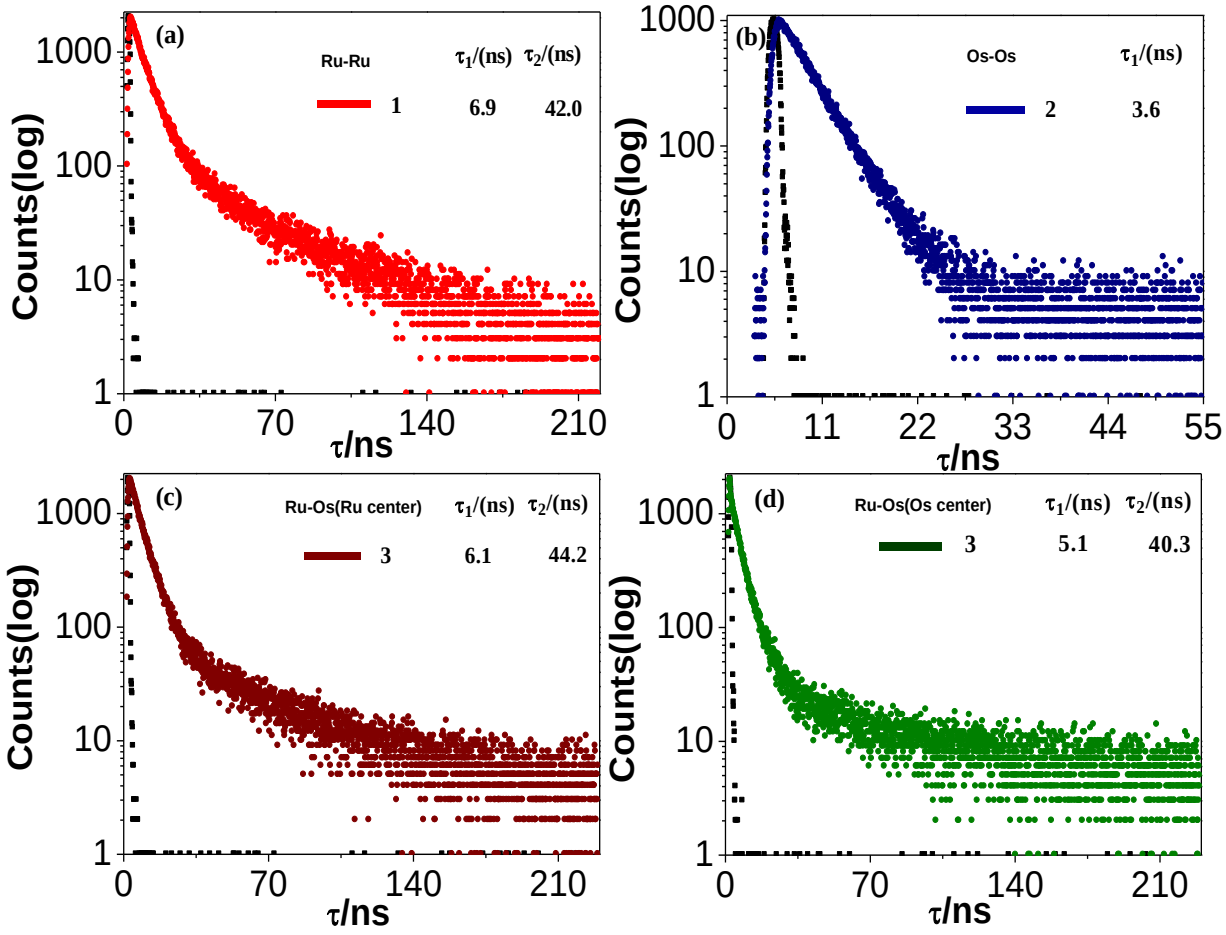

Figure S7. Time resolved emission spectra of **1-3** in their free state in acetonitrile solution.

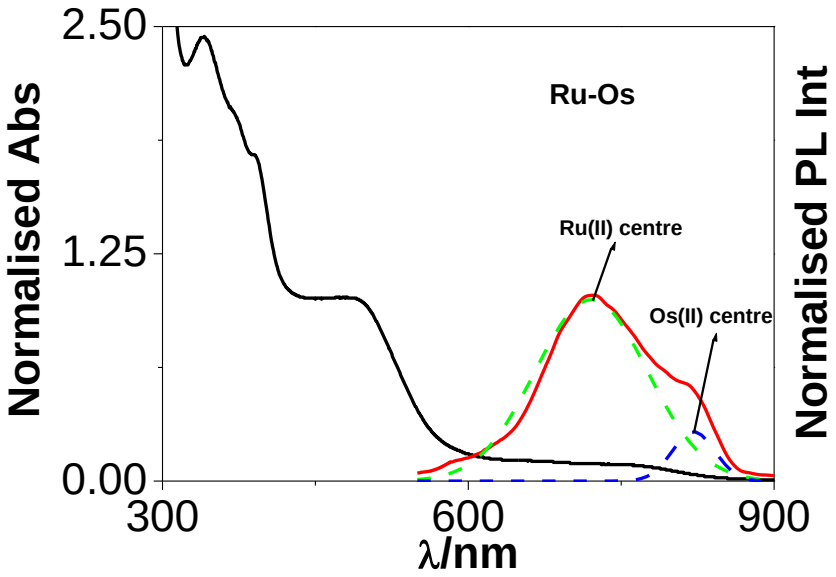

Figure S8. Overlay of normalized absorption and emission spectra of the hetero dimmer **3**. Dotted lines indicate the deconvoluted emission spectra of **3**.

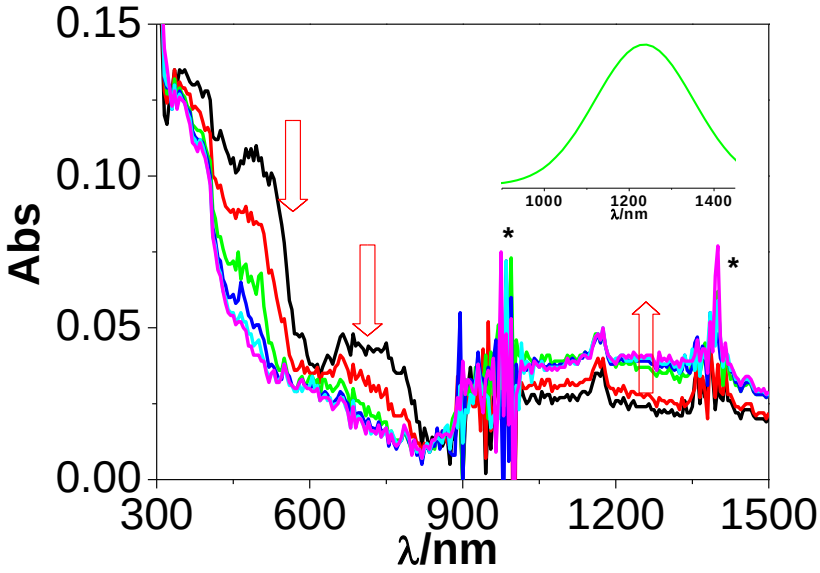

Figure S9. Spectroelectrochemical changes during the oxidation of $[(bpy)_2Os(Py\text{-}Biimz)Os(bpy)_2]^{2+}$ (**2**) in acetonitrile. The IVCT band obtained from spectral deconvolution is shown in the inset. Asterisks denote artefacts due to non-perfect back ground compensation.

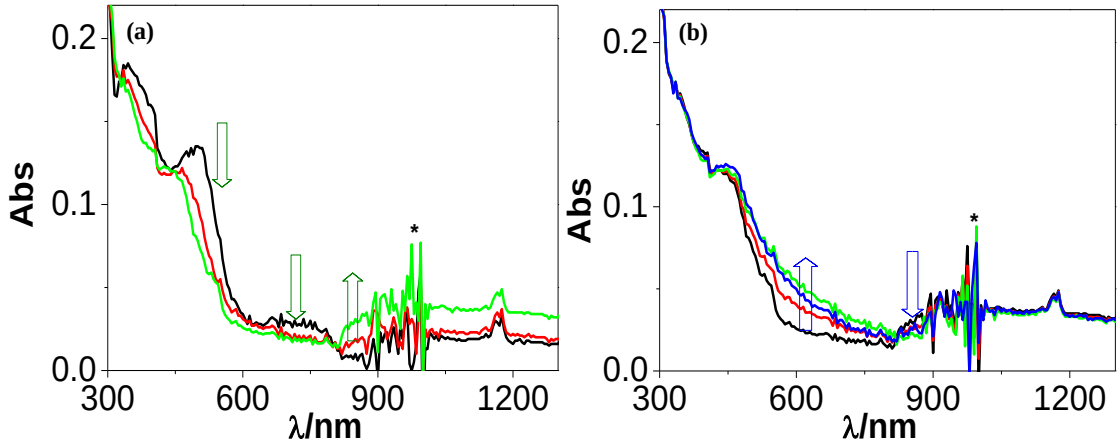

Figure S10. Spectroelectrochemical changes during the oxidation of $[(bpy)_2Ru(Py\text{-}Biimz)Os(bpy)_2]^{2+}$ (**3**) in acetonitrile. Asterisks denote artefacts due to non-perfect back ground compensation.

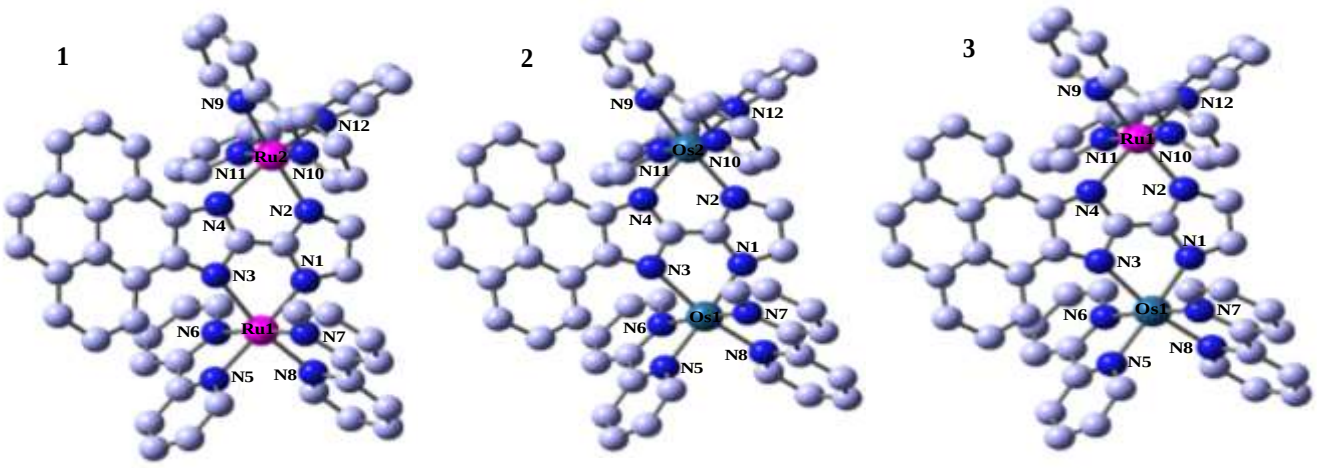

Figure S11. Optimized geometries and labelling scheme for $[(bpy)_2Ru(Py\text{-}Biimz)Ru(bpy)_2]^{2+}$ (**1**)**,** $[(bpy)_2Os(Py\text{-}Biimz)Os(bpy)_2]^{2+}$ (**2**) and $[(bpy)_2Ru(Py\text{-}Biimz)Os(bpy)_2]^{2+}$ **(3)** in solution phase.

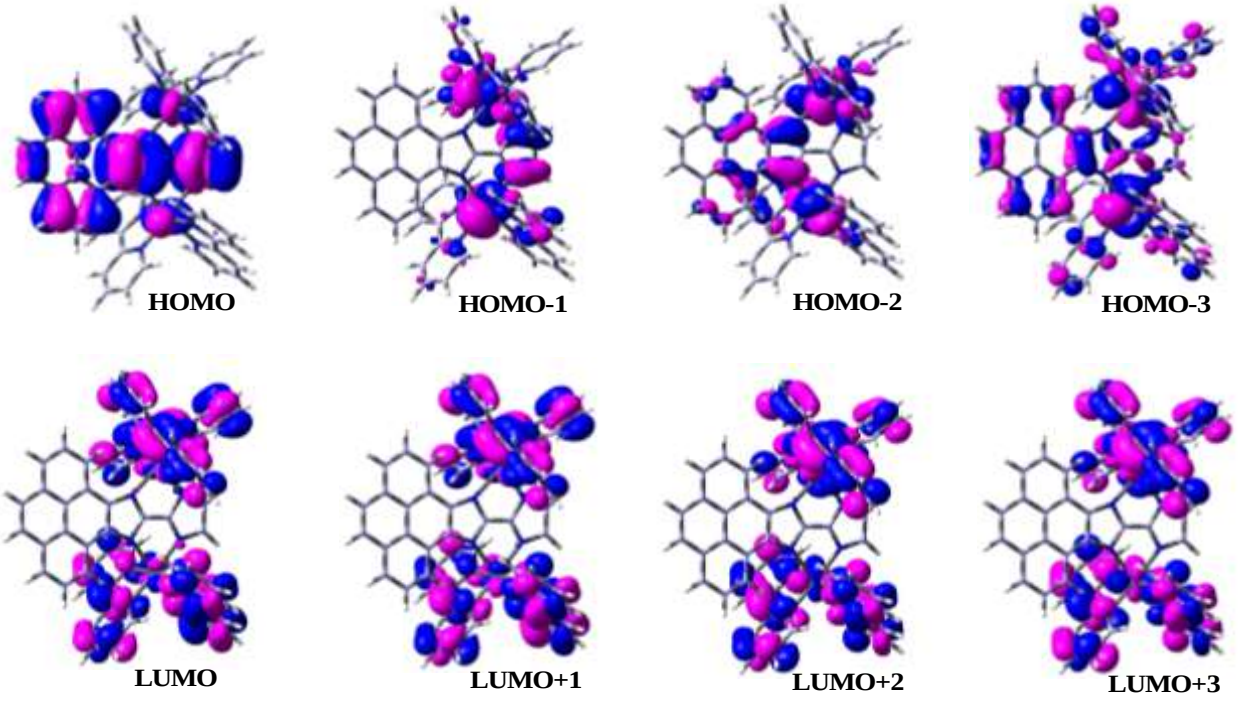

Figure S12. Schematic drawings of the selective frontier molecular orbitals for $[(bpy)_2Os(Py\text{-}Biimz)Os(bpy)_2]^{2+}$ (**2**) in acetonitrile.

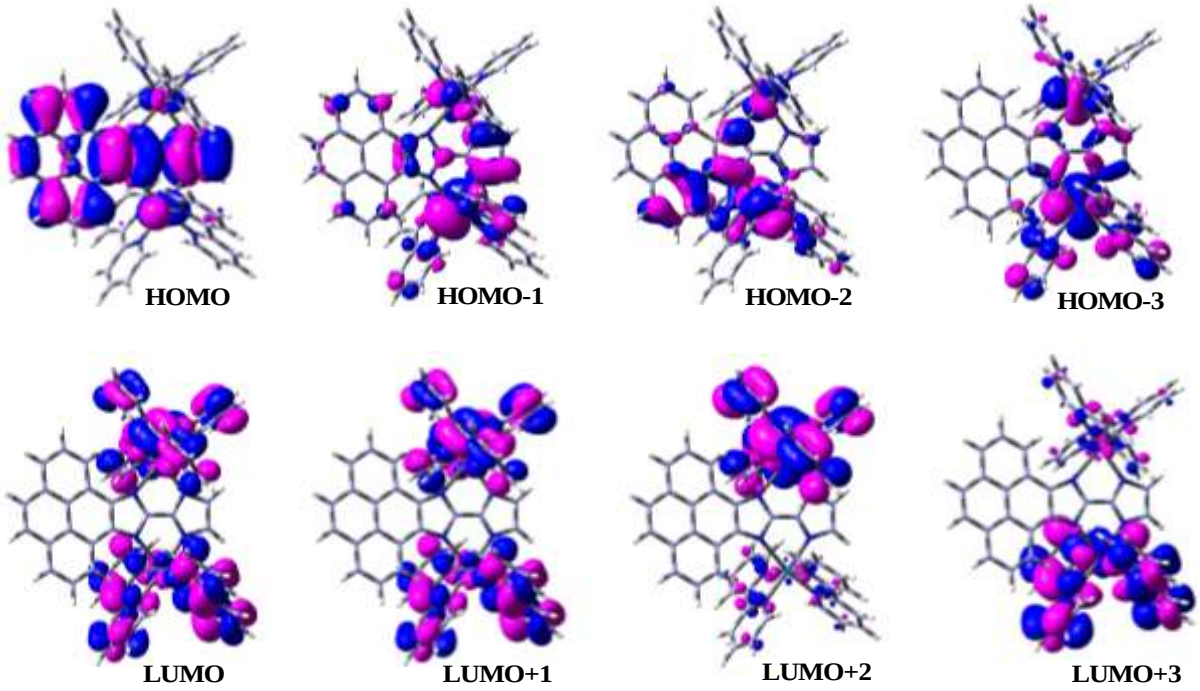

Figure S13. Schematic drawings of the selective frontier molecular orbitals for $[(bpy)_2Ru(Py\text{-}Biimz)Os(bpy)_2]^{2+}$ (**3**) in acetonitrile.

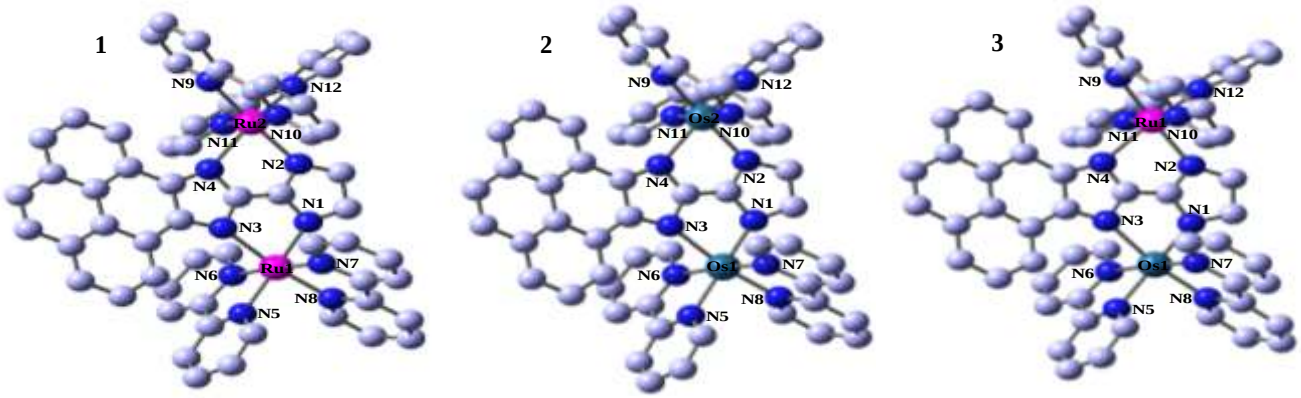

Figure S14. UKS optimized geometries and labelling scheme for $[(bpy)_2Ru(Py\text{-}Biimz)Ru(bpy)_2]^{2+}$ (**1**), $[(bpy)_2Os(Py\text{-}Biimz)Os(bpy)_2]^{2+}$ (**2**) and $[(bpy)_2Ru(Py\text{-}Biimz)Os(bpy)_2]^{2+}$ **(3)** in acetonitrile.

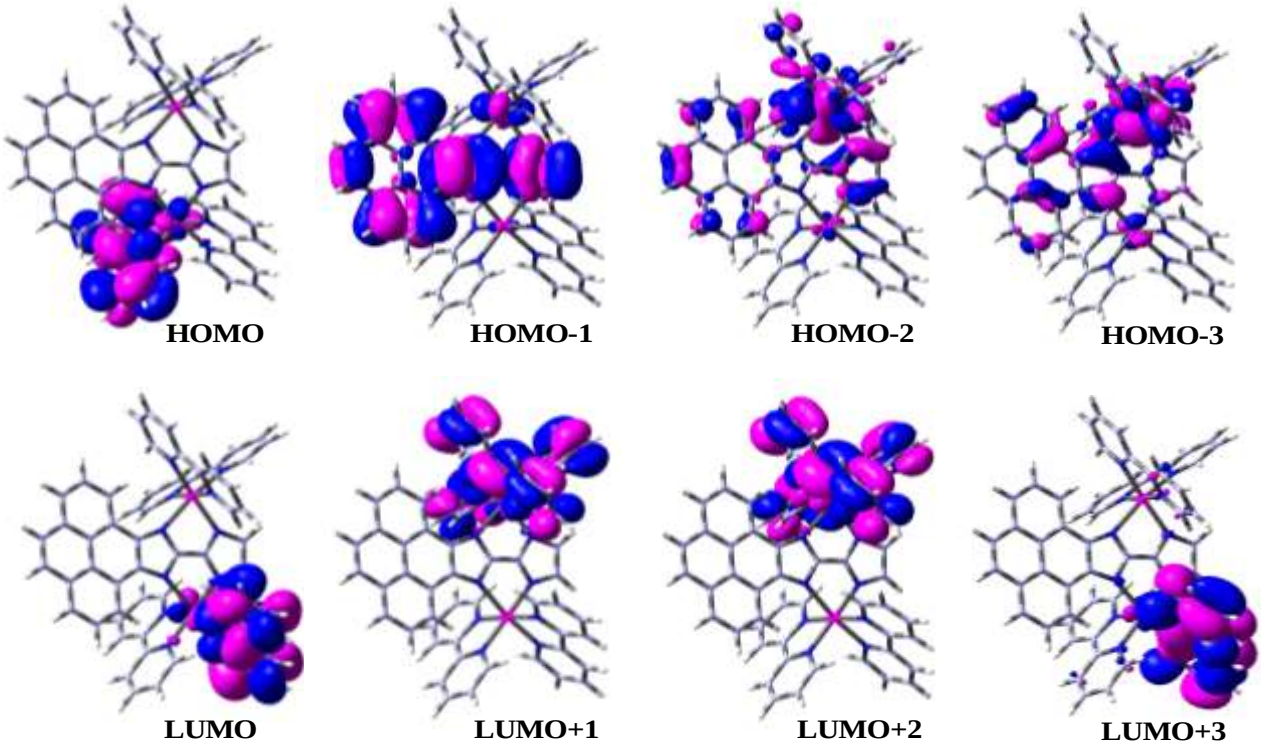

Figure S15. Schematic drawings of the selective frontier molecular orbitals for $[(bpy)_2Ru(Py\text{-}Biimz)Ru(bpy)_2]^{2+}$ (**1**) in UKS optimized state.

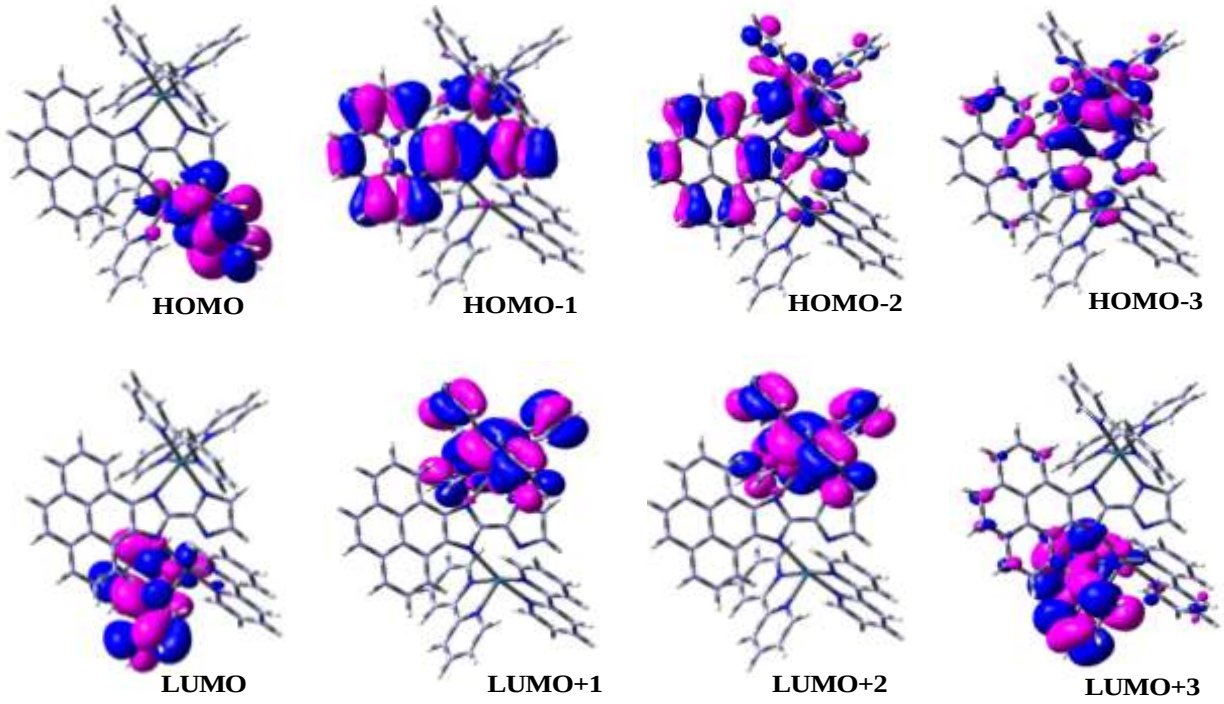

Figure S16. Schematic drawings of the selective frontier molecular orbitals for $[(bpy)_2Os(Py\text{-}Biimz)Os(bpy)_2]^{2+}$ (**2**) in UKS optimized state.

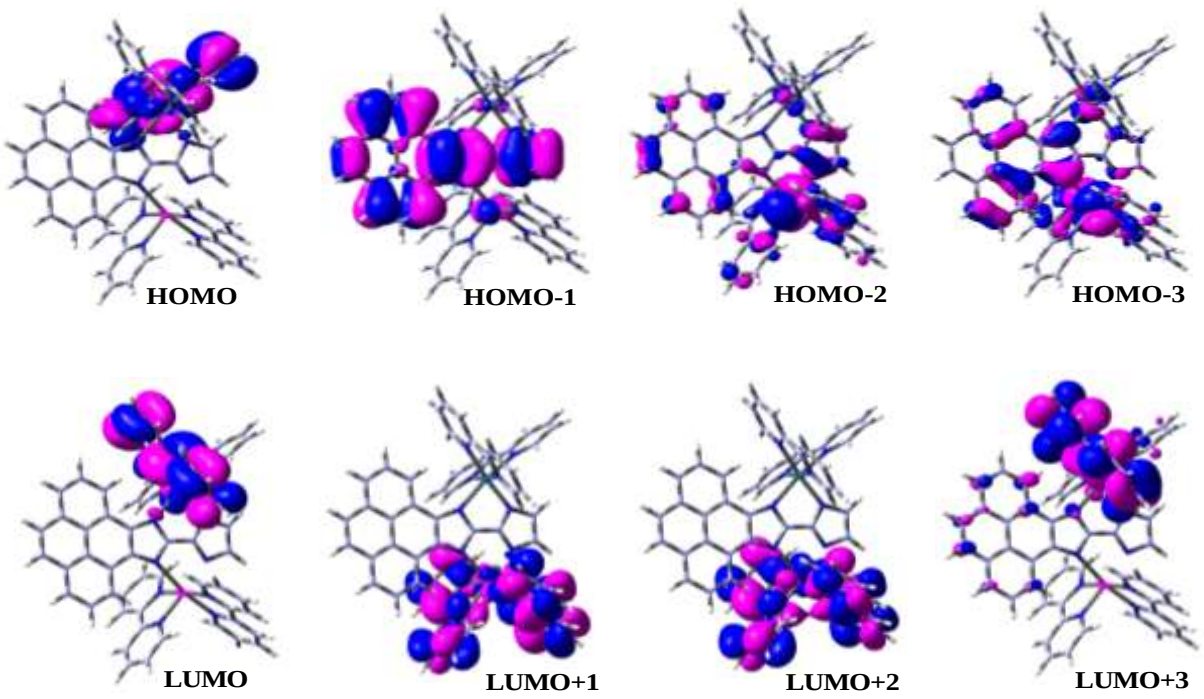

Figure S17. Schematic drawings of the selective frontier molecular orbitals for $[(bpy)_2Ru(Py\text{-}Biimz)Os(bpy)_2]^{2+}$ (**3**) in UKS optimized state.

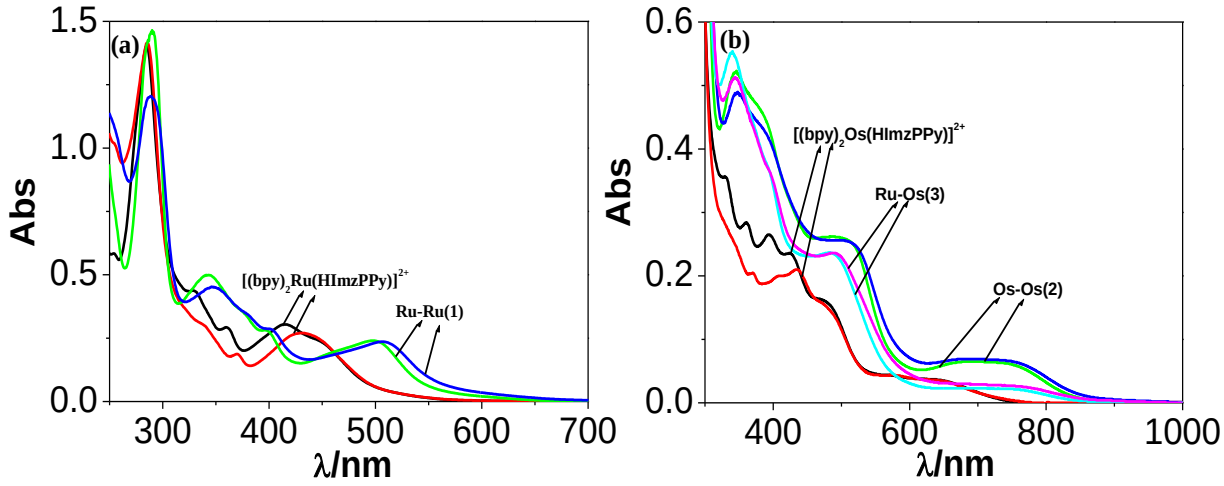

Figure S18. Overlayed absorption spectra of $[(bpy)_2M(HImzPPy)]^{2+}$ and $[(bpy)_2M/M_1(Py\text{-}Biimz)M/M_2(bpy)_2]^{2+}$ systems in presence of DNA.

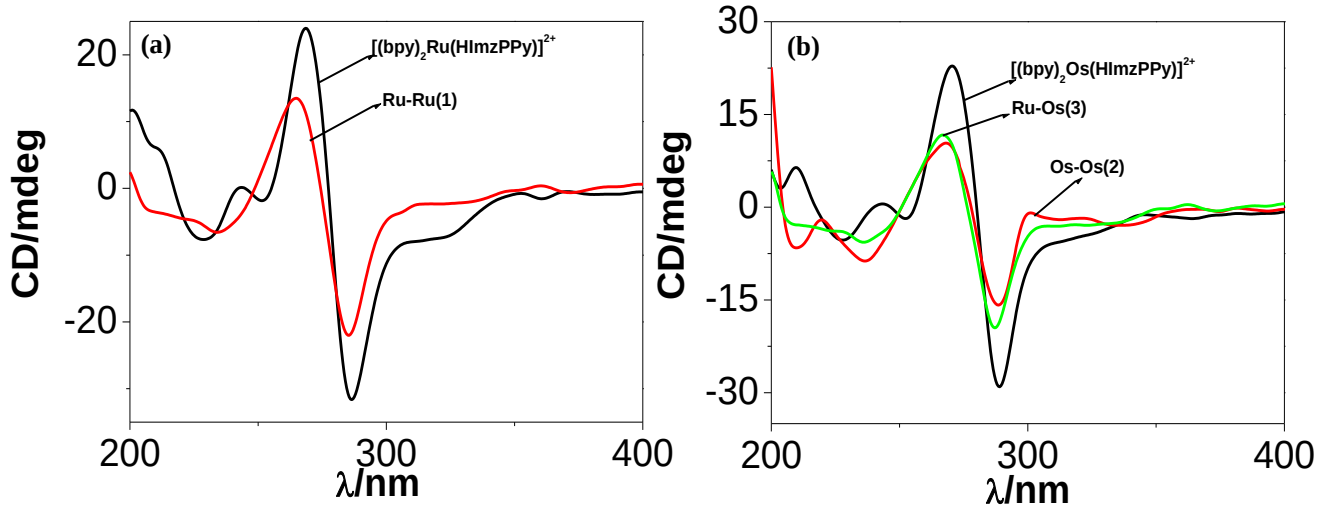

Figure S19. Overlayed CD spectra of $[(bpy)_2M(HImzPPy)]^{2+}$ and $[(bpy)_2M/M_1(Py\text{-}Biimz)M/M_2(bpy)_2]^{2+}$ systems in presence of DNA.

References

(S1) (a) Nair, R. B.; Teng, E. S.; Kirkand, S. L.; Murphy, C. J. *Inorg. Chem.* **1998**, *37*, 139. (b) Nair, R. B.; Murphy, C. J. *J. Inorg. Biochem.* **1998**, *69*, 129.

(S2) (a) Cater, M. T.; Rodriguez, M.; Bard, A. J. *J. Am. Chem. Soc*. **1989**, *111*, 8901. (b) Smith, S. R.; Neyhart, G. A.; Karlsbeck, W. A.; Thorp, H. H. *New. J. Chem.* **1994**, *18*, 397.

(S3) Boger, D. L.; Fink, B. E.; Brunette, S. R.; Tse, W. C.; Hedrick, M. P. *J. Am. Chem. Soc.***2001**, *123*, 5878.

(S4) SAINT (version 6.02), SADABS (version 2.03); Bruker AXS Inc.: Madison, WI, **2002**.

(S5) SHELXTL, (version 6.10); Bruker AXS Inc.: Madison, WI, **2002**.

(S6) Sheldrick, G. M. SHELXL-97, *Program for the Refinement of crystal Structures*; University of Göttingen: Göttingen, Germany, **1997**.

(S7) PLATON; Spek, A. L. *J. Appl. Cryst.* **2003**, *36*, 7-13.

(S8) Frisch,M. J.; Trucks, G. W.; Schlegel, H. B.; Scuseria, G. E.; Robb, M. A.; Cheeseman, J. R.; Scalmani, G.; Barone, V.; Mennucci, B.; Petersson, G. A.; Nakatsuji, H.; Caricato, M.; Li, X.; Hratchian, H. P.; Izmaylov, A. F.; Bloino, J.; Zheng, G.; Sonnenberg, J. L.; Hada, M.; Ehara, M.; Toyota, K.; Fukuda, R.; Hasegawa, J.; Ishida, M.; Nakajima, T.; Honda, Y.; Kitao, O.; Nakai, H.; Vreven, T.; Jr. Montgomery, J. A., Peralta, J. E.; Ogliaro, F.; Bearpark, M.; Heyd, J. J.; Brothers, E.; Kudin, K. N.; Staroverov, V. N.; Kobayashi, R.; Normand, J.; Raghavachari, Rendell, K. A.; Burant, J. C.; Iyengar, S. S.; Tomasi, J.; Cossi, M.; Rega, N.; Millam, J. M.; Klene, M.; Knox, J. E.; Cross, J. B.; Bakken, V.; Adamo, C.; Jaramillo, J.; Gomperts, R.; Stratmann, R. E.; Yazyev, O.; Austin, A. J.; Cammi, R.; Pomelli, C.; Ochterski, J. W.; Martin, R. L.; Morokuma, K.; Zakrzewski, V. G.; Voth, G. A.; Salvador, P.; Dannenberg, J. J.; Dapprich, S.; Daniels, A. D.; Farkas, Ö.; Foresman, J. B.; Ortiz, J. V.; Cioslowski, J.; Fox, D. J. Gaussian 09, revision A.02; Gaussian Inc.: Wallingford, CT, **2009**.

(S9) Becke, A. D. *J. Chem. Phys.* **1993**, *98*, 5648-5652.

(S10) Lee, C. T.; Yang, W. T.; Parr, R. G. *Phys. Rev. B* **1988**, *37*, 785-789.

(S11) (a) Andrae, D.; Haeussermann, U.; Dolg, M.; Stoll, H.; Preuss, H. *Theor. Chim. Acta.* **1990**, *77*, 123. (b) Fuentealba, P.; Preuss, H.; Stoll, H.; Szentpaly, L. V. *Chem. Phys. Lett*. **1989**, *89*, 418.

(S12) Hay, P. J.; Wadt, W. R. *J. Chem. Phys.* **1985**, *82*, 299-310.

(S13) Casida, M. E.; Jamorski, C.; Casida, K. C.; Salahub, D. R. *J. Chem. Phys.* **1998**, *108*, 4439-4449.

(S14) Stratmann, R. E.; Scuseria, G. E.; Frisch, M. J. *J. Chem. Phys.* **1998**, *109*, 8218-8224.

(S15) Walters, V. A.; Hadad, C. M.; Thiel, Y.; Colson, S. D.; Wiberg, K. B.; Johnson, P. M.; Foresman, J. B. *J. Am. Chem. Soc.* **1991**, *113*, 4782-4791.

(S16) (a) Tomasi, J.; Mennucci, B.; Cammi, R. *Chem. Rev*. **2005**, *105*, 2999−3094. (b) Cossi, M.; Scalmani, G.; Rega, N.; Barone, V. *J. Chem. Phys*. **2002**, *117*, 43−54.

(S17) Caricato, M.; Mennucci, B.; Tomasi, J.; Ingrosso, F.; Cammi, R.; Corni, S.; Scalmani, G. *J. Chem. Phys*. **2006**, *124*, 124520-124533.

(S18) Mennucci, B.; Cappelli, C.; Guido, C. A.; Cammi, R.; Tomasi, J. *J. Phys. Chem. A* **2009**, *113*, 3009-3020.

(S19) Dennington, R. II.; Keith T.; Millam, J. *Gauss View 3*; Semichem, Inc.: Shawnee Mission, KS, **2007**.

(S20) O Boyle, N. M.; Tenderholt, A. L.; Langner, K. M. *J. Comput. Chem*. **2008**, *29*, 839-845.